JOURNAL OF Applied Polymer SCIENCE

# The Effects of Gas Counter Pressure and Mold Temperature Variation on the Surface Quality and Morphology of the Microcellular Polystyrene Foams

**Shia-Chung Chen,[1,2,3] Ping-Shun Hsu,[1,2,3] Shyh-Shin Hwang[4]**

[1]Department of Mechanical Engineering, Chung Yuan Christian University, Taiwan
[2]R&D Center for Mold and Molding Technology, Chung Yuan Christian University, Taiwan
[3]R&D Center for Membrane Technology, Chung Yuan Christian University, Chung-Li, Taiwan
[4]Department of Mechanical Engineering, Ching-Yun University, Taiwan

Correspondence to: S.-C. Chen (E-mail: shiachun@cycu.edu.tw)

**ABSTRACT:** In this study, we developed a foaming control system using the Gas Counter Pressure (GCP) combined with mold temperature control during the microcellular injection molding (MuCell) process and investigated its influence on the parts' surface quality and foams structures. The results revealed that under GCP control alone when GCP is greater than 10 MPa, part surface roughness for transparent polystyrene (PS) improved by 90%. When GCP increased, the skin thickness also increased, the weight reduction decreased and the average cell size reduced to about 30 $\mu$m. For black PS parts, when GCP is greater than 10 MPa, the part gloss reaches the same value as that molded by conventional injection molding. By increasing gas holding time, the cell density decreased and the cell size distribution became more uniform. The increase in amount of supercritical fluid foaming agent also increased the cell density. Applying mold temperature control alone with temperature in the range of 90–120°C (near $T_g$), the surface roughness improved by 65%. Increasing mold temperature decreased the skin thickness; however, the cell size distribution became significantly nonuniform. It was found that thin skin, small and uniform cell size as well as good surface quality can be achieved efficiently by simultaneous combining of GCP and mold temperature control. The proposed innovative approach may lead to a significant improvement and a more broad application for MuCell process. © 2012 Wiley Periodicals, Inc. J. Appl. Polym. Sci. 000: 000–000, 2012

**KEYWORDS:** microcellular injection molding; gas counter pressure; mold temperature control; surface roughness; cell size; foam structure

Received 15 October 2011; accepted 2 May 2012; published online
**DOI: 10.1002/app.37994**

## INTRODUCTION

Microcellular foaming technology of polymers was developed about three decades ago.[1,2] In 1982, Mrtini et al. investigated the foaming of PS in solid state using gas as blowing agent in a batch process. In 2001, Trexel Inc. successfully developed a microcellular injection molding process and named the process as MuCell.[3] The supercritical fluids (SCF) used in the MuCell process have characteristics of gas-like diffusivity, low viscosity, and liquid-like density. MuCell offers many advantages, such as shrinkage reduction, warpage minimization, light weight, lower melt viscosity, and elimination of sink marks. Relevant studies on the process characteristics and molded part properties have been reported.[3–9] The most difficult issue that opposes MuCell's wide application is silver-like swirl flow marks appearing on part surface during the melt-filling process.

Several methods have been proposed to improve the surface roughness of MuCell parts, including control of SCF content,[10] material modification, In-Mold Decoration (IMD) process to have decorated film on part surface, and coinjection molding process leading to a solid skin and microcellular foamed core.[11] Dynamic mold temperature control[12–14] using coated surfaces or film-insert mold surface by delaying heat transfer on the cavity surface leads to an elevated mold temperature during melt-filling stage. Another possibility of solving the surface quality issue is counter pressure techniques, particularly the gas counter pressure (GCP) process[15–20] that has been reported to effectively improve the part surface roughness. Bledzki et al.[19] reported a reduction of the part surface roughness (Rz) from 23 $\mu$m to 0.85 $\mu$m. Although the preliminary studies of GCP with MuCell process were carried out recently, the systematic and more

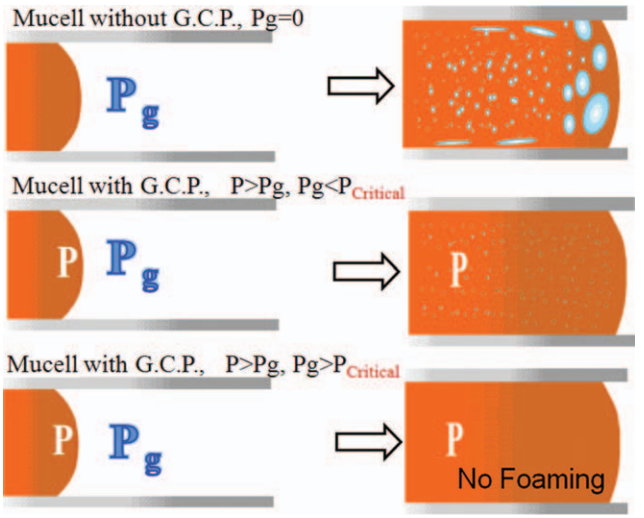


**Figure 1.** Effects of GCP control on the foams structures.[20] [Color figure can be viewed in the online issue, which is available at wileyonlinelibrary.com.]

detailed investigations are necessary. The main effect of GCP is described in Figure 1. In a typical MuCell process, when melt filling starts, the low pressure around melt front leading to SCF foaming and the foaming bubbles are brought to the part surface by fountain flow. When the SCF dissolves in the polymer, and the melt advances against a counter pressure in the melt front, three phenomena may occur. If the counter pressure is zero or one atmosphere, free foaming occurs during the melt filling stage that usually leads to a silver-strike like flow mark on the part surface. If counter pressure is greater than one atmosphere and less than the critical pressure required for maintaining the nitrogen as SCF, the foaming will be restricted. If the gas counter pressure is higher than the critical pressure, then the melt may retain as a single phase without any foaming as long as the counter pressure applies. A more detailed recent study[20] reported that when the gas counter pressure is greater than a certain value, a foaming free part surface may be produced. In addition, gas holding time after melt filling also assists foaming restriction and results in no foaming if long gas holding is employed. The other successful case was that using GCP to measure the melt viscosity dissolved with SCF.[21]

In this study, a new concept of P-T path control method was applied in foaming quality control of MuCell parts (Figure 2). Earlier studies on foaming control follow either by varying temperature alone[9–11] or by varying pressure alone[12–17] independently. Our study proposed that an approach of simultaneous control of both pressure and temperature and hope this can effectively improve the foaming process. Therefore, a GCP combined with mold temperature system was established. The system consists of four main units (a) a typical MuCell injection system; (b) a mold designed with proper sealing and installed with gas injection/release valves allowing high pressurized gas being injected/released from the mold cavity; (c) process signal measuring system; and (d) mold temperature control system using two coolant temperature control units, as shown in Figure 3. In this way, not only a bubble free and solid surface can be achieved, the foams structures, including cell size and cell density, can also be well controlled.

## EXPERIMENTAL

An Arburg 420C Allrounder 1000-350 injection molding machine equipped with a MuCell supercritical fluid system was used to control the process and the products structures. A GCP gas control unit installed with a high frequency gas control valve connected to the mold was used to adjust and monitor the real time gas pressure inside the mold cavity, as shown in Figure 4. Furthermore, a mold temperature control unit was provided by two-mold temperature control units, one was used for rapid heating and the other was utilized for rapid cooling, as shown in Figure 5. A schematic drawing of the slit cavity design, which was used in this work, is shown in Figure 6. The cavity has dimensions of 100 mm (length), 30 mm (width), and 3 mm (thickness). Part thickness of 3 mm is chosen because it represents a typical thickness for MuCell molding. Besides, the chosen thickness is also appropriate to investigate the variation of foaming along the thickness direction. To measure the real time pressure and temperature in the cavity during the MuCell with GCP process, two pressure sensors were installed in the cavity side and two temperature sensors were embedded in the core side. A high temperature seal was used to prevent gas leakage from the mold cavity.

A transparent general purpose polystyrene resin (POLYREX PG-33, CHIMEI Chemicals) was used in this study. Nitrogen was used as the SCF blowing agent and GCP gas source. Relevant molding conditions of MuCell with GCP combined with the mold temperature control are presented in Table I. Transparent PS allows one easily to identify visually the foaming situation. In P-T path control method, variations of GCP (5, 10, and 15 MPa), holding times (0, 3, and 5 s), and mold temperature (60, 90, and 120°C) under SCF level 0.5 wt % was applied in MuCell process. In our earlier study,[20] the applied counter pressure was varied within a range of 0 to 30 MPa. The critical pressure that restricts foaming was found to be 10 MPa. In this study, we choose GCP range below and above 10 MPa. Figure 7 illustrates the real time monitored curves of pressure and temperature variations in the mold cavity during the MuCell

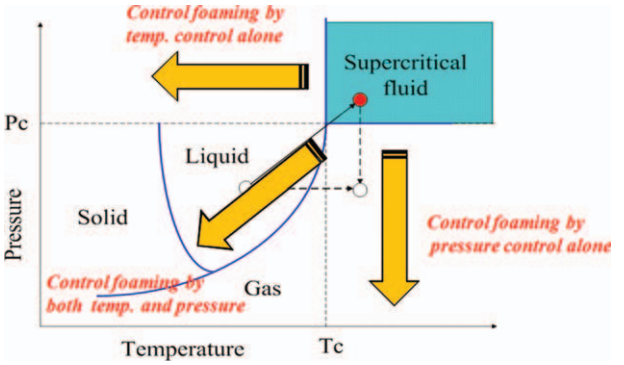


**Figure 2.** Concept of foam structure control via P-path alone, T-path alone, and a combined P-T Path. [Color figure can be viewed in the online issue, which is available at wileyonlinelibrary.com.]

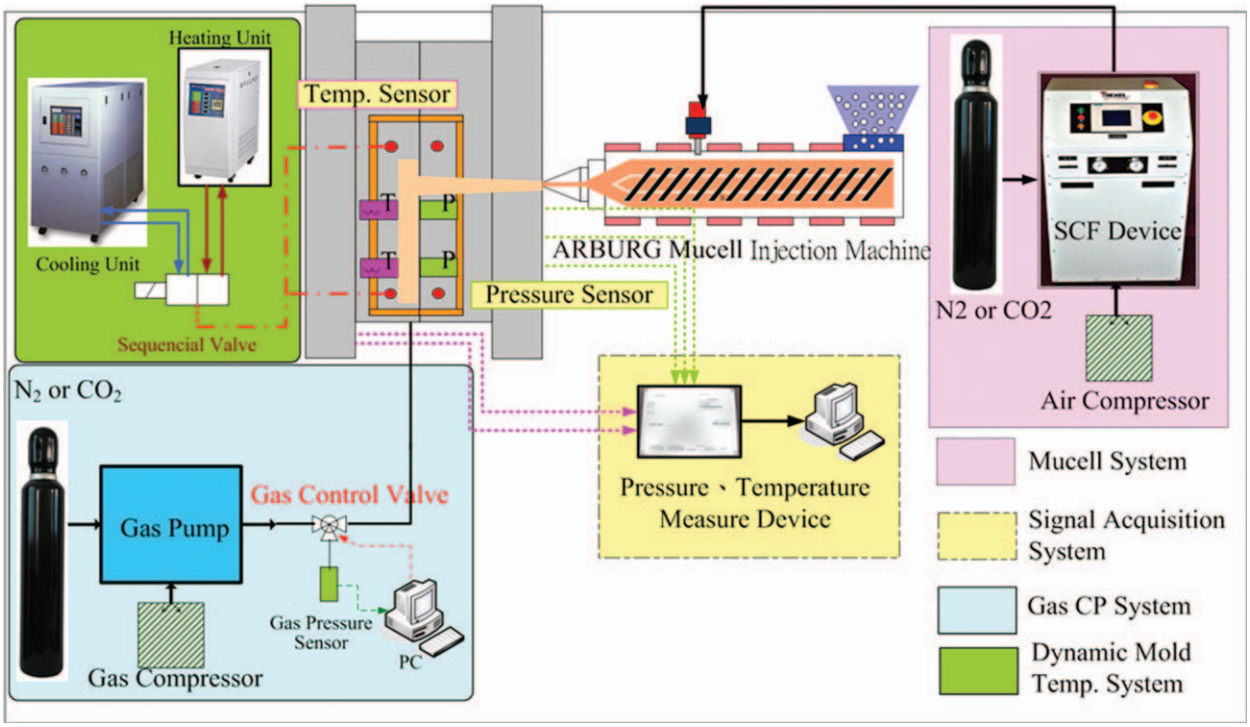


**Figure 3.** Schematic design of MuCell injection molding with GCP control and mold temperature control systems. [Color figure can be viewed in the online issue, which is available at wileyonlinelibrary.com.]

process. It shows that a sufficient, stable, and high response GCP was used in the system. More detailed cavity gas pressure monitoring prior and after melt injection can be seen in Figure 6 of Ref. 20. The measured cavity pressure during melt filling will be higher than the gas counter pressure. At the end of melt filling, the cavity pressure will drop to the same value as that of gas counter pressure. At the end of melt filling, mold temperature was also decreased. Surface roughness was measured by 3D laser microscope (Keyence VK8550). A typical example can be seen in Figure 12 of an earlier study.[20] Morphology of foamed cell were examined by Scanning Electron Microscope (SEM), from which solid skin layer thickness, averaged foamed size as well as cell density can be calculated. Finally, black PS was also used to verify the surface gloss situation for MuCell parts when compared with that of conventional injection molding (CIM). The surface gloss measurement follows ASTM D523-85 standard, using BYK micro-TRI-gloss$\mu$. This cosmetic issue is rather important for molded parts.

## RESULTS AND DISCUSSION

The foaming part becomes opaque because the foam bubbles scatter the light. The less the foaming caused the samples to be

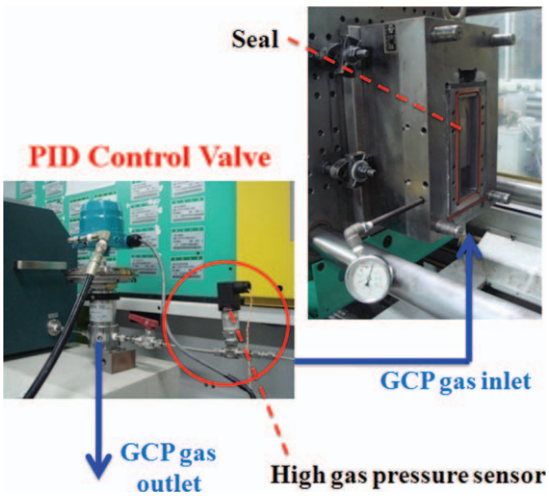


**Figure 4.** GCP control system.[20] [Color figure can be viewed in the online issue, which is available at wileyonlinelibrary.com.]

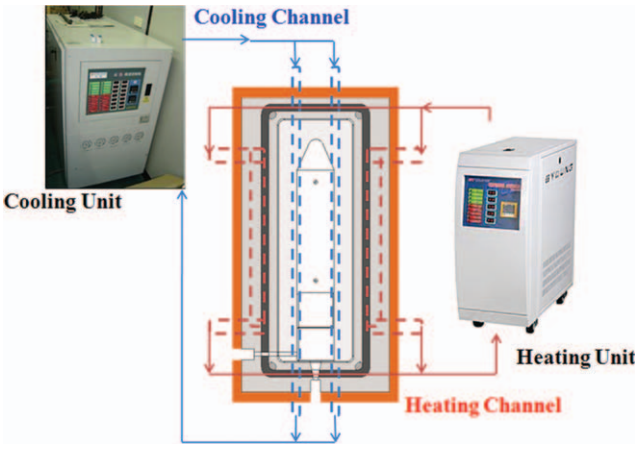


**Figure 5.** Design of mold temperature control unit. [Color figure can be viewed in the online issue, which is available at wileyonlinelibrary.com.]

Applied Polymer SCIENCE

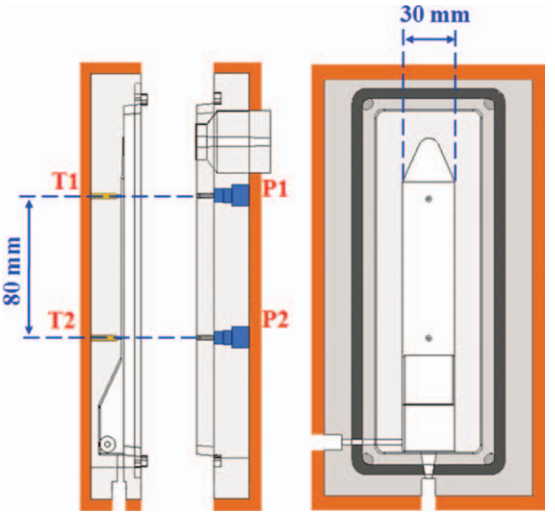


**Figure 6.** Slit cavity size and sensors positions.[20] [Color figure can be viewed in the online issue, which is available at wileyonlinelibrary.com.]

more transparent. At the end of the melt filling stage, when counter pressure was suddenly released, foaming immediately started. The cooling starts after the end of melt filling. As a result, the cooling proceeds in the gas holding stage as shown in the temperature profiles of Figure 7. However, because the part surface solidified, the foaming occurred only within the melt core, resulting in a transparent and shiny skin and a foamed core. Side views of the MuCell parts under GCP control are shown in Figure 8. It is clear to see that at high gas holding time, the foaming has been completely restricted resulting in fully transparent parts.

**Table I.** Conditions of MuCell Process

| Material | PS (amorphous) |
|---|---|
| Injection velocity (mm/s) | 5 |
| Part thickness (mm) | 3 |
| Initial mold temp. (°C) | 40 |
| Melt temp. (°C) | 210 |
| SCF level (wt %) | 0.5 |
| SCF flow rate (kg/h) | 0.30 |
| Conditions of GCP control | |
| Valve gate delay time (s) | 5 |
| GCP (MPa) | 5, 10, 15 |
| Gas holding time (s) | 0, 3, 5 |
| Conditions of mold temperature control | |
| Mold temperature (°C) | 60, 90, 120 |
| Cooling water temperature(°C) | 8 |

The location of MuCell parts which were examined by SEM and a typical side view of the foam cellular structure are shown in Figure 9(a,b), respectively. The comparisons of surface roughness of MuCell parts under GCP, and mold temperature control as well as GCP combined with mold temperature control are shown in Figure 10. From the results, it can be found that under the condition of GCP alone and GCP combined with mold temperature control, the surface roughness can achieve an improvement ratio of greater than 90%. Under the mold temperature control alone, when the mold temperature varied in the range of 90–120°C (near $T_g$), the surface roughness improved by over 65%.

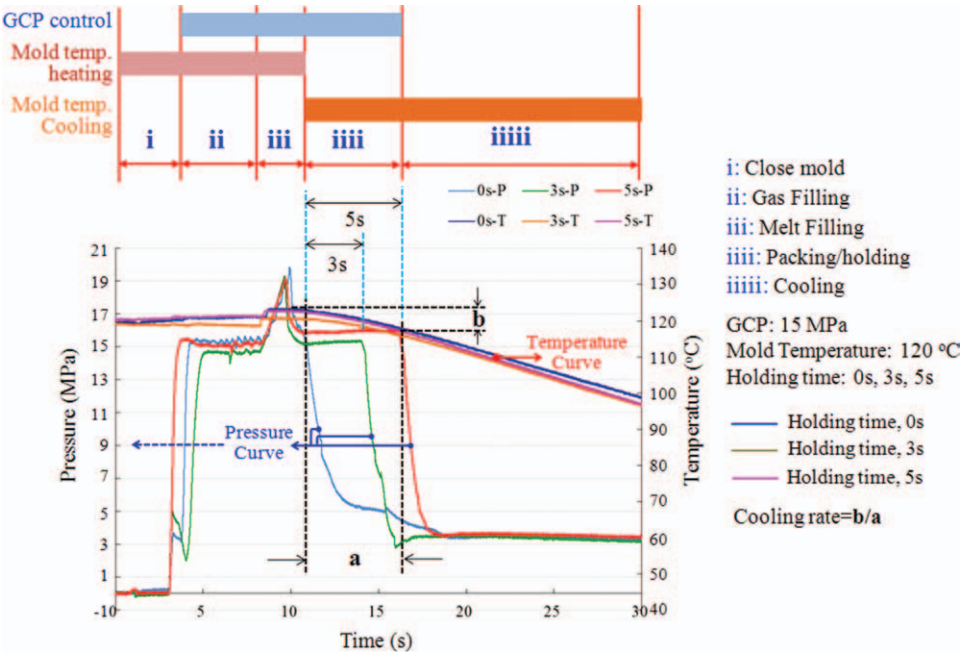


**Figure 7.** Real-time mold pressure and temperature acquisition inside the mold cavity at GCP 15 MPa with 0, 3, and 5 s gas holing time; initial mold temperature is 120°C; various stages of process operation are also designated on the top. [Color figure can be viewed in the online issue, which is available at wileyonlinelibrary.com.]

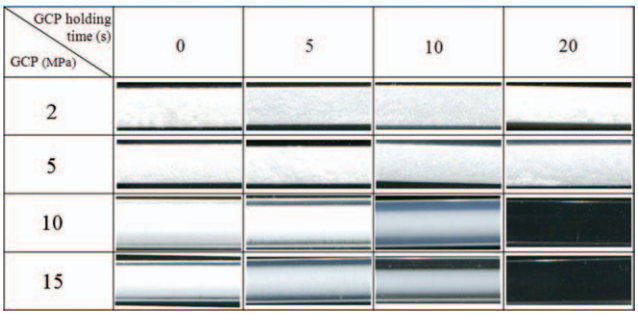


**Figure 8.** Side view of MuCell parts under GCP control. [Color figure can be viewed in the online issue, which is available at wileyonlinelibrary.com.]

Figure 11 shows the cross section views of the SEM micrographs of samples produced at different foaming conditions. The foams structures indicate different skin layers and cell size distributions under GCP and mold temperature control. For MuCell parts molded applying GCP alone, the skin thickness increases with increased GCP value. For mold temperature control alone, skin thickness of MuCell part decreases with increased mold temperature meanwhile cell size increases and some cells even become undesired voids. Combined with GCP and mold temperature, it is clearly seen in the photos of bottom row that MuCell parts achieve thinner skin and more fine cell size when GCP is about 10 MPa and mold temperature is around 120°C. When GCP is

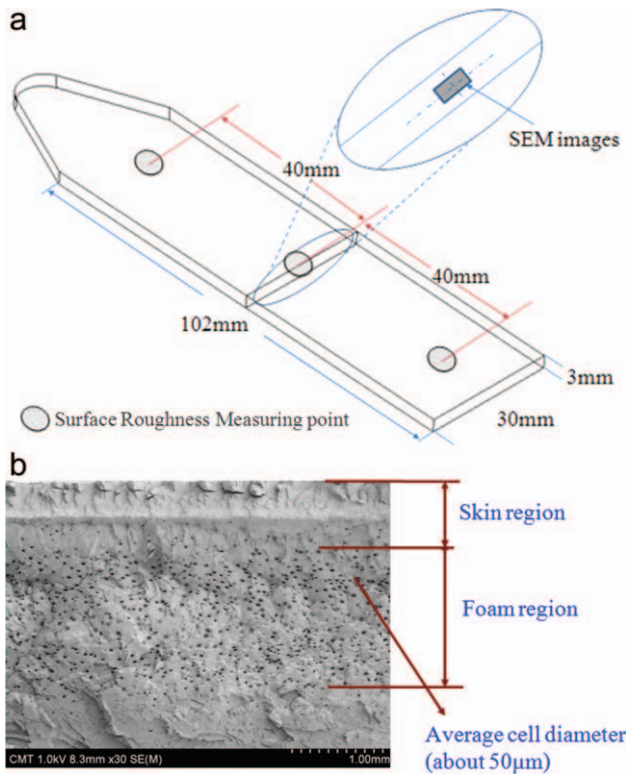


**Figure 9.** a: Examination locations for part foaming status; b: a typical SEM micrograph of a foamed sample cross section at GCP 10 MPa without gas holding time (averaged cell size is about 50 $\mu$m). [Color figure can be viewed in the online issue, which is available at wileyonlinelibrary.com.]

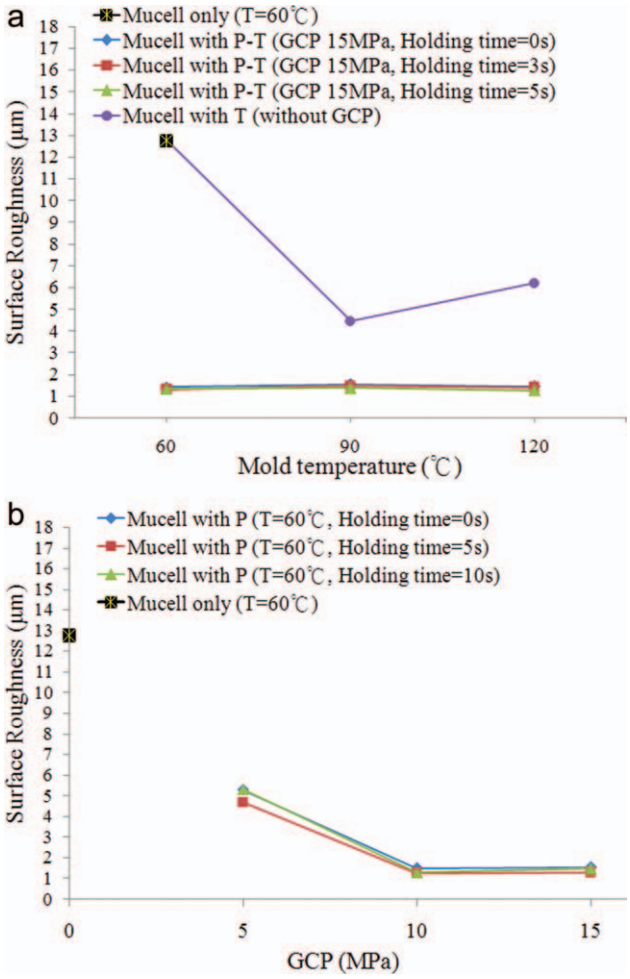


**Figure 10.** Comparisons of surface roughness under (a) various mold temperature and (b) various GCP. [Color figure can be viewed in the online issue, which is available at wileyonlinelibrary.com.]

lower than 10 MPa foaming begins during injection phase, the partial free foaming leads to larger cell size. When GCP is much greater than 10 MPa, the foaming is severely restricted resulting in smaller cell size and low cell density. Figures 12–14 show the cell size, the skin thickness, and the cell density of the foams samples in different conditions of GCP control alone, dynamic mold temperature control alone, and combined GCP with the mold temperature controls. When GCP alone increased from 2 to 15 MPa, the skin thickness increased from 292 to 690 $\mu$m with no gas holding time, the weight reduction ratio decreased and the average cell size also reduced to about 30 $\mu$m. On the other hand, when the mold temperature alone increased, the skin thickness decreased to 200 $\mu$m and the cell size distribution was significantly nonuniform. In a combined GCP and temperature control process (simultaneous P-T path), the produced foams had low skin thickness, more uniform and smaller cell sizes, and higher cell density. The further concern of part surface is gloss issue. Weight reduction ratio of MuCell parts when compared with regular CIM parts are also shown in Figure 15. It was found in this study that weight reduction is not only

Applied Polymer SCIENCE

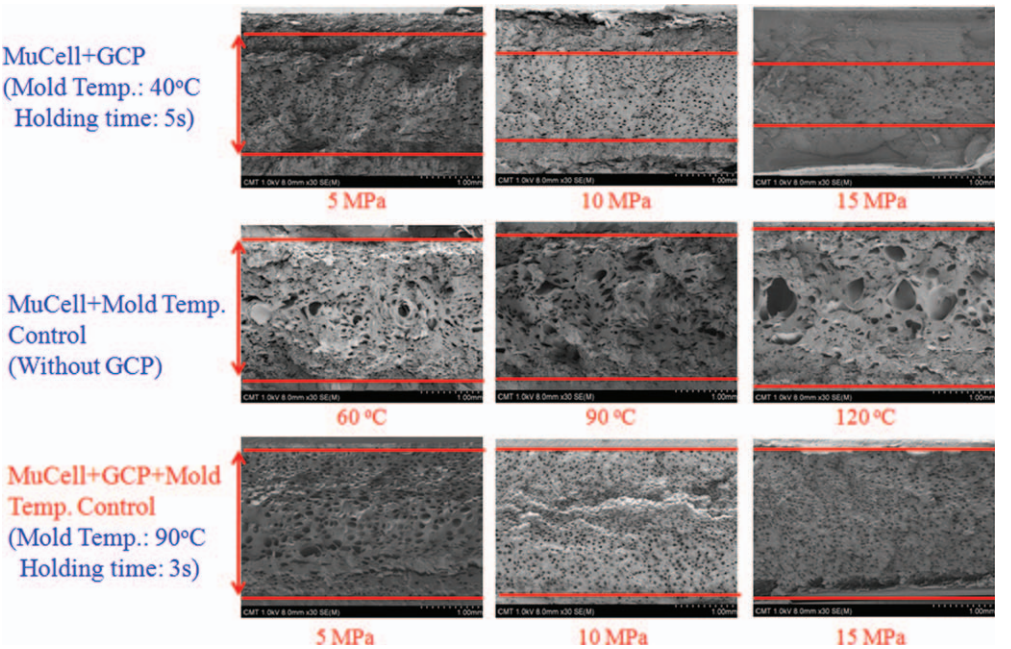


**Figure 11.** Comparisons of foam morphologies using GCP control, mold temperature control, and GCP combined with mold temperature control. [Color figure can be viewed in the online issue, which is available at wileyonlinelibrary.com.]

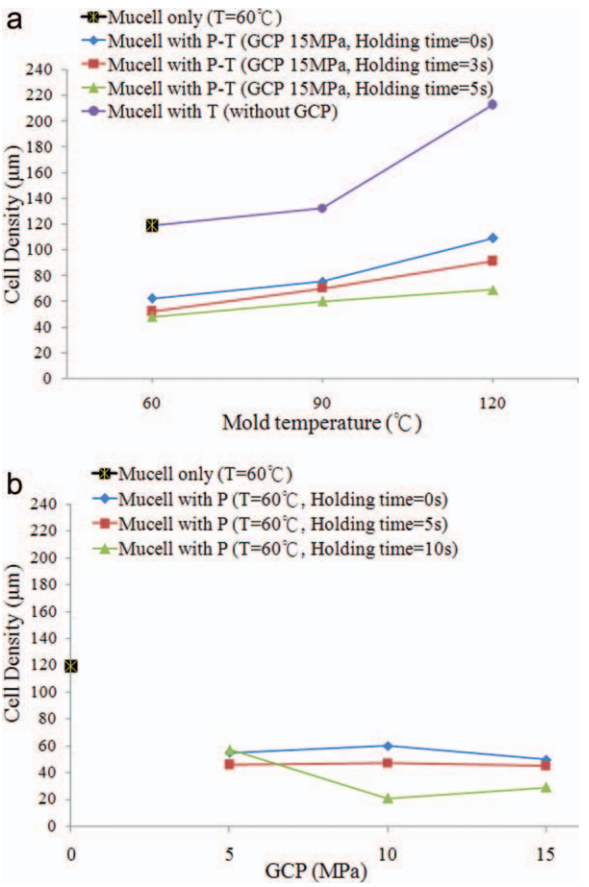


**Figure 12.** Comparison of the cell sizes under (a) various mold temperature and (b) various GCP. [Color figure can be viewed in the online issue, which is available at wileyonlinelibrary.com.]

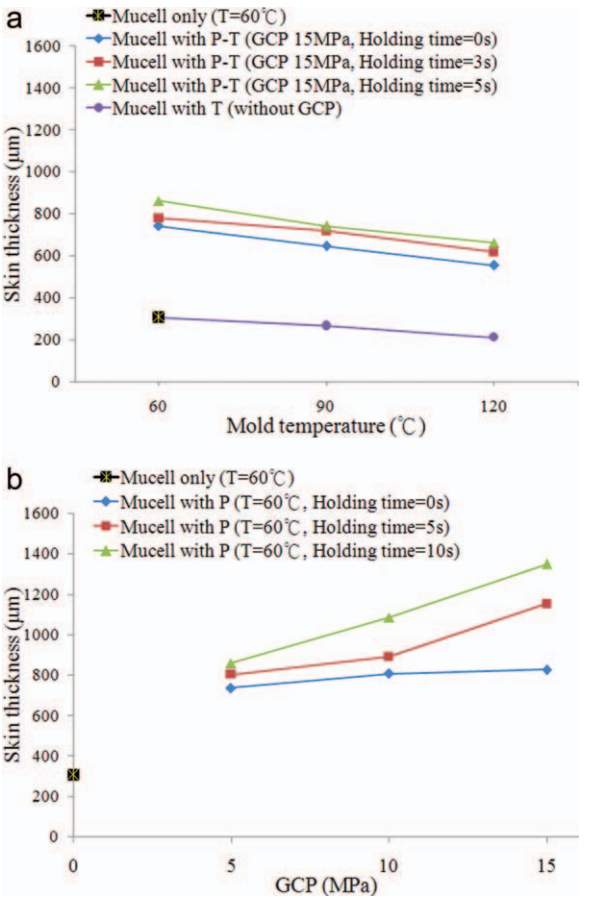


**Figure 13.** Comparison of the skins thicknesses under (a) various mold temperature and (b) various mold temperature. [Color figure can be viewed in the online issue, which is available at wileyonlinelibrary.com.]

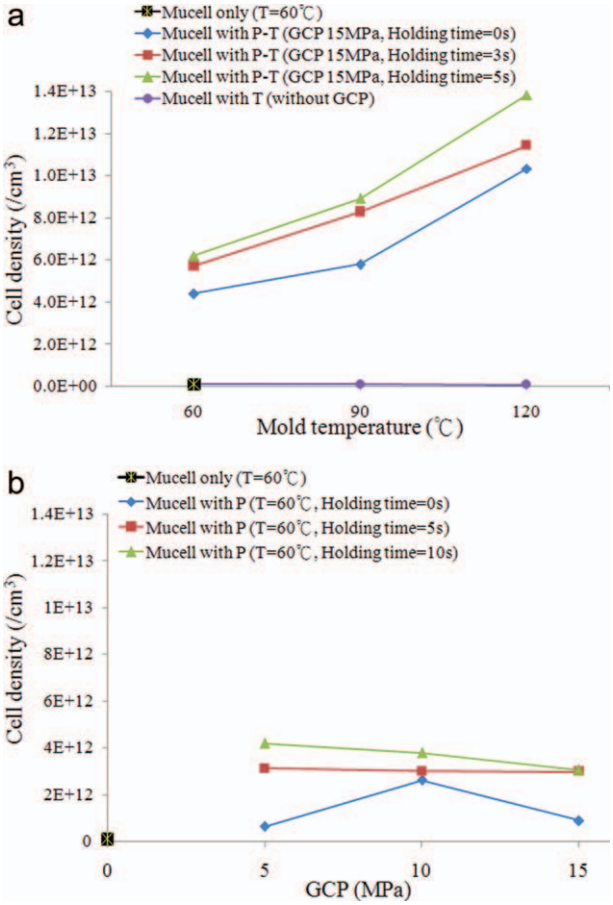


**Figure 14.** Comparison of the cell densities under (a) various mold temperature and (b) various GCP. [Color figure can be viewed in the online issue, which is available at wileyonlinelibrary.com.]

related to cell size and cell density but also to the skin thickness (no foaming region). As result, weight reduction is not a monotonous relation with cell size and/or cell density. Figure 16 shows the MuCell process for black PS parts. When GCP is greater than 10 MPa, the gloss value of the part surface exhibits

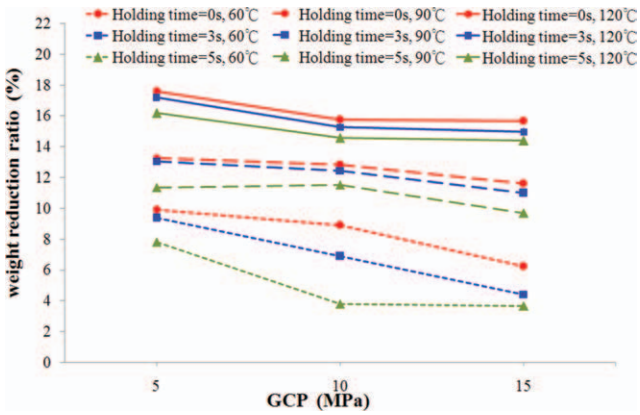


**Figure 15.** Comparison of the weight reduction ratio under various GCP and different mold temperature of 60, 90, and 120°C. [Color figure can be viewed in the online issue, which is available at wileyonlinelibrary.com.]

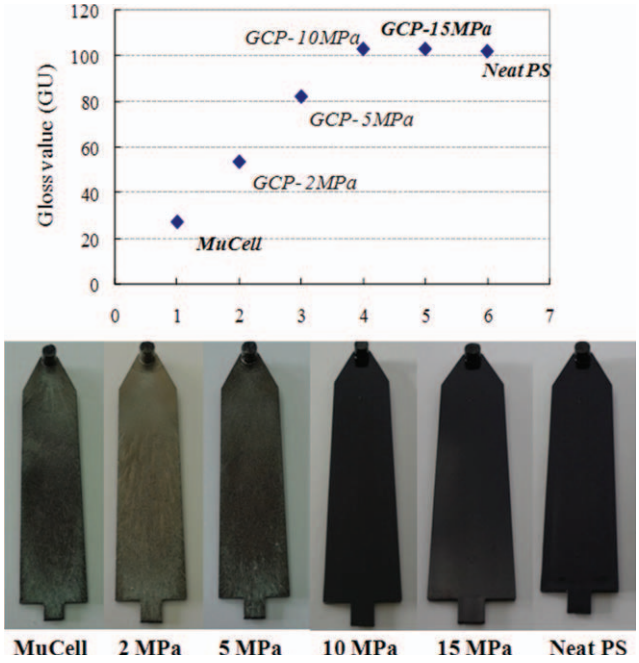


**Figure 16.** Gloss values and surface appearance of black PS MuCell parts under various GCP. [Color figure can be viewed in the online issue, which is available at wileyonlinelibrary.com.]

almost the same value as that molded by conventional injection. This further verifies that the part surface is foaming-free. With the same surface quality for MuCell part as that of CIM part, it certainly enhances the application potential for MuCell process.

## CONCLUSIONS

In this study, a new method of P-T path control was developed for improving both surface quality and foam structure. We successfully established a GCP control combined with mold temperature control system which can not only supply gas counter pressure up to 30 MPa, but it can provide a reasonable response in the pressure setup, the cooling rate of the mold temperature control system reached 1°C/s. Effects of various gas counter pressures, holding times and mold temperatures and their effects on the foams structures and part surface quality were investigated. It was found that although employing GCP alone can restrict bubble formation at the part surface leading to surface quality improvement, however, the skin thickness also increased with increasing GCP. Increasing mold temperature alone results in thinner skin but the foamed cell size becomes larger and unevenly distributed. Combining with GCP and mold temperature simultaneously, molded MuCell parts and thin skin, defect-free surface with small and uniform cell size were produced. The proposed approach enhances the application potential for MuCell process significantly.

## ACKNOWLEDGMENTS

This research was financially supported from the Ministry of Economic Affairs, the National Science Council, the Ministry of Education, and R&D Center for Membrane Technology of Taiwan, ROC.

## REFERENCES


1. Martini, J.; Waldman, F.; Suh, N. P. *SPE ANTEC Tech. Papers* **1982,** *28*, 674.
2. Suh, N. P. Microcellular Plastics. In J. F., Ed.; Hanser Publishers: Munich, **1996;** p 93.
3. Xu, J.; Pierick, D. *J. Injection Molding Technol.* **2001,** *5*, 152.
4. Gong, W.; Gao, J.; Jiang, M.; He, L.; Yu, J.; Zhu, J. *J. Appl. Polym. Sci.* **2011,** *122*, 2907.
5. Kaewmesri, W.; Rachtanapun, P.; Pumchusak, J. *J. Appl. Polym. Sci.* **2008,** *107*, 63.
6. Huang, H. X.; Wang, J. K. *J. Appl. Polym. Sci.* **2007,** *106*, 505.
7. Goel, D. I.; Baird, D. G. *Polym. Eng. Sci.* **1995,** *35*, 1167.
8. Kumar, V. *SPE ANTEC Tech. Papers* **2002,** *60*, 1892.
9. Collias, D. I.; Baird, D. G. *Polym. Eng. Sci.* **1995,** *35*, 1167.
10. Lee, J.; Turng, L. S. *Polym. Eng. Sci.* **2010,** *50*, 1281.
11. Turng, L. S.; Khabas, H. *Int. Polym. Process.* **2004,** *19*, 77.
12. Chen, H. L.; Chien, R. D.; Chen, S. C. *Int. Commun. Heat Mass Transfer* **2008,** *35*, 991.
13. Chen, S. C.; Lin, Y. W.; Chien, R. D.; Li, H. M. *Adv. Polym. Technol.* **2008,** *27*, 224.
14. Cha, S. W.; Yoon, J. D. *Polym-Plast. Technol. Eng.* **2005,** *44*, 795.
15. Semerdjiev, S. VEB Deutscher Verlag für Grundstoffindustrie, **1980.**
16. Bledzki, A. K.; Kirschling, H.; Steinbichler, G.; Egger, P. Trans Tech Publication: Zurich, Switzerland, **2005;** p 257.
17. Michaeli, W.; Opfermann, D. *SPE ANTEC Tech. Papers* **2006,** *64*, 1290.
18. Yoon, J. D.; Hing, S. K.; Kim, J. H.; Cha, S. W. *Cell. Polym.* **2004,** *23*, 39.
19. Bledzki, A. K.; Kirschling, H.; Steinbichler, G.; Egger, P. *J. Cell. Plast.* **2004,** *40*, 489.
20. Chen, S. C.; Hsu, P. S.; Lin, Y. W. *Int. Polym. Process.* **2011,** *26*, 275.
21. Chen, S. C.; Chung, M. H.; Lin, Y. W.; Hsu, P. S.; Hwang, S. S.; Hsu, P. M. *e-Polymers* **2010,** *128*, 1.